

1  
2  
3  
4  
5  
6  
7  
8  
9  
10  
11  
12  
13  
14  
15  
16  
17  
18  
19  
20  
21  
22  
23

## **Softwood-lignin/natural rubber composites containing novel plasticizing agent: Preparation and characterization**

Janusz Datta\*, Paulina Parcheta, Joanna Surówka

Gdańsk University of Technology, Faculty of Chemistry, Department of Polymers Technology, G. Narutowicza Str. 11/12, 80-233 Gdańsk, Poland

\*Corresponding author (J. Datta): [janusz.datta@pg.gda.pl](mailto:janusz.datta@pg.gda.pl)

ABSTRACT: Composite materials based on natural rubber were obtained by using glycerolysate (decomposition product of polyurethane) as a novel plasticizer. In order to determine the effect of various lignin content, four different filler amounts were used, namely 5 phr (parts per 100 parts of natural rubber) of lignin (WLI5G), 10 phr of lignin (WLI10G), 20 phr (WLI20G), and 40 phr (WLI40G). The reference specimen without lignin (WLI0G) was also prepared. The resulting vulcanizates were analyzed by Fourier Transform Infrared Spectroscopy (FTIR) to determine the chemical interaction between the lignin powder and the natural rubber chain. The SEM analysis of the cross-sections of the obtained materials was carried out to determine the adhesion between lignin and rubber. The results of dynamic mechanical analysis (DMA) and thermogravimetric analysis (TGA) showed that the samples containing 5 and 10 phr of lignin had the best thermal properties. Also, the measured mechanical properties, such as tensile strength, hardness, resilience and abrasiveness, confirmed these findings.

KEYWORDS:

Softwood Lignin;

- 24 Natural rubber composites;
- 25 Scanning Electron Microscopy;
- 26 Thermal analysis;
- 27 Mechanical properties;
- 28 Equilibrium swelling measurements

29

## 30 **1. INTRODUCTION**

31 At present, many scientific teams work on the possibility to employ natural  
32 resources in the field of materials science and engineering. It is a consequence of the  
33 ending stocks of petrochemical resources such as coal, natural gas, and crude oil.  
34 One of the most important issues related to green chemistry is the utilization of  
35 renewable resources as a new application in the existing products. Moreover, the  
36 polymer recycling process and the utilization of polymer recycling products constitute  
37 the second most urgent task due to the increase in the waste quantity. It has been  
38 proven that the renewables and the products of polymer recycling can partially  
39 replace the primary resources used in the polymer synthesis and preparation. The  
40 resulting materials display the same, approximately the same, or even better  
41 properties.

42 One of the most recent issues in green chemistry is finding the possibility to  
43 maximize the application of lignin by-products, which are produced in vast amounts  
44 by the paper and pulp industries, in the field of polymer technology. Presently, ca. 50  
45 million tons of lignin by-products produced annually by the industries are used as a



46 fuel for the energy production (Faruket al., 2016a). Only 2 % of this valuable raw  
47 material is used for other applications because of the complex structure and  
48 heterogeneity of lignin, which causes difficulties during delignification on a  
49 commercial scale that is conducted by the pulp and paper industries (DeWild et al.,  
50 2014; Neutelings, 2011).

51 Lignin is a highly branched bio-macromolecule. It is composed of units such as  
52 paracoumaryl alcohol, coniferyl alcohol and sinapyl alcohol (Jianget al., 2014). These  
53 phenylpropane units have none, one, or two methoxyl groups at the positions 3 or 5  
54 in the phenolic ring (Faruket al., 2016a). The aforementioned molecules are linked  
55 together by different bond types, i.e. 5-O-4,  $\beta$ -O-4,  $\beta$ -1,  $\beta$ -5,  $\beta$ - $\beta$ , etc. (Rogers, 2015).  
56 Chakar et al. (Chakarand Ragauskas, 2004) presented the percentages of different  
57 bonds in softwood lignin,  $\beta$ -O-4 being the most common one. This particular bond  
58 type is present in up to 50 % of total bonds in softwood-lignin.

59 The varying occurrence of bond types depends on the origin of lignin, i.e. the  
60 sources of softwood or hardwood, which results in different percentages of bond  
61 content. Bjornsson indicated that generally hardwoods contain less lignin than  
62 softwoods (Bjornsson, 2014). The exact lignin structure not only depends of the type  
63 of biomass, but also of the type of delignification process used, which modifies lignin  
64 to a certain degree (Hatakeyama and Hatakeyama, 2010). The application of various  
65 delignification methods results in a variety of lignin products. The main types of lignin  
66 can be divided into liginosulfonates, kraft lignin, and organosolv lignin (Holladay et al.,  
67 2007).

68 The delignification process affects the content of impurities in the obtained  
69 products and, consequently, their further applicability. Liginosulfonates can be used

70 as dispersants, emulsion stabilizer, carbon black, industrial binders, agricultural  
71 chemicals or concrete additives due to their medium purity (residual sulfur). Kraft  
72 lignin also contains some ash and sulfur, and can be used as emulsifiers,  
73 dispersants, carbon fibers or binders. Organosolv lignin, which is sulfur free, has the  
74 highest degree of purity. Because of this property, it is possible to use organosolv  
75 lignin for the synthesis of aromatic polyols, new diacids, carbon fibers, activated  
76 carbon, phenolic resins, phenol derivatives and antioxidants (Faruket al., 2016a;  
77 Holladay et al., 2007).

78 Plasticizers, represented by freely available, non-volatile compounds, are  
79 widely used in the polymer production due to the important role they play in the  
80 resulting products. They improve processability during the polymer preparation as  
81 well as add flexibility to the final materials (Vieiraet al., 2011). Over the past years,  
82 due to the increasing interest of polymer industries in biopolymers, biorenewables  
83 and the products of the chemical recycling of polymer waste, many publications  
84 appeared in which the addition of a biopolymer plasticizer and/or biodegradable  
85 plasticizing materials of natural origin had been described. Altenhofen Da Silva and  
86 co-workers utilized the product of the polyesterification of rice fatty acid as a  
87 plasticizer in the poly(vinyl chloride) and natural rubber films. The results of this  
88 research indicate that the addition of natural plasticizer increased the elongation at  
89 break compared to pure polymer film. In terms of thermogravimetric analysis no  
90 significant differences were detected between the plasticized material and pure  
91 natural rubber-based product (Altenhofen Da Silva et al., 2011). Alexander and  
92 Thachil investigated differences between cardanol and aromatic oil employed as  
93 plasticizers. It was demonstrated that cardanol, used as a plasticizing agent in the  
94 natural-rubber matrix, gave mechanical properties similar to those obtained with the

95 aromatic oil-based materials (Alexander and Thachil, 2006). The same observation  
96 was later reported by Mohapatra and Nando (Mohapatra and Nando, 2014).

97         The main aim of this research was to prepare and characterize natural rubber-  
98 based composites filled with various amounts of lignin, and obtained with the use of  
99 glycerolysate. This experimental set up was an exemplification of the application of  
100 the chemical recycling of polymer product as a novel plasticizer in the natural rubber  
101 matrix. The synthesis of the plasticizer used in our study had been based on the  
102 decomposition of polyurethane waste by means of chemicals, heat and catalysts.  
103 Polyurethanes are in the sixth place in the ranking of the most used polymers in the  
104 global market. The polyurethane waste constitutes ca. 6 % of all plastic waste  
105 (Kopczyńska and Datta, 2016). As a result, the chemical recycling processes of  
106 polyurethanes are one of the most prolific development tasks in the materials  
107 engineering (Simonet al., 2014). Moreover, the most investigated are the wastes of  
108 flexible polyurethane foams due to their extensive application and the resulting high  
109 volume of waste that entails environmental and economic problems (Nikjeand Nikrah,  
110 2007). Glycerolysate is the product of thermo-mechanical recycling of polyurethane,  
111 with the use of glycerine as a decomposition prime mover. The process is called  
112 glycolysis or glycerolysis, and it is the transesterification reaction between hydroxyl  
113 groups in glycol or glycerol (glycerine), respectively, which interchanged the ester  
114 groups in the polyurethane chains (Simónet al., 2016). The decomposition product of  
115 polyurethane is a mixture of compounds and monomers. Until now, glycerolysates  
116 were most frequently used to synthesize polyurethanes, mainly in the form of foams  
117 (Simónet al., 2016) or elastomers (Datta,2010; Datta and Pasternak, 2005), in which  
118 polyols were partially or completely replaced by the product of the chemical recycling  
119 of polyurethane.

120 This paper describes novel elastic composites containing four different levels  
121 of lignin, and the same amount of plasticizer in the form of glycerolysate. The  
122 influence of lignin content on the structure, morphology, and the selected  
123 mechanical, thermal and chemical properties of the obtained composites was  
124 investigated.

## 125 **2. EXPERIMENTAL**

### 126 **2.1. MATERIALS**

127 Natural rubber used to prepare the composites was purchased from Torimex  
128 Chemicals Ltd Sp. z o. o., KonstantynówŁódzki, Poland (density  $0.92 \text{ g/cm}^3$ , weight  
129 average molecular weight,  $M_w = 800\,000 \text{ mol/g}$ ). Lignin (INDULIN AT – kraft pine  
130 lignin – softwood lignin) used in this study was obtained from MeadWestvaco  
131 Corporation, Specialty Chemical Division, South Carolina, USA. INDULIN AT with a  
132 density of ca.  $1.25 \text{ g/cm}^3$  was dried prior to use at  $100^\circ\text{C}$  for 12 hours in air. After  
133 drying, it was applied as a filler in the rubber mix. Sulfur with a density of about 1.8-  
134  $2.1 \text{ g/cm}^3$  and a molecular weight of  $32.1 \text{ g/mol}$  was also purchased from Torimex  
135 Chemicals Ltd Sp. z o. o. Other ingredients, listed below, were purchased from  
136 BrenntagPolska Sp. z o. o., Kędzierzyn - Koźle, Poland:

- 137 • stearic acid with a density of about  $0.85 - 0.99 \text{ g/cm}^3$  and a molecular weight  
138 of  $284.5 \text{ g/mol}$ ,
- 139 • zinc oxide with a density of about  $5.6 \text{ g/cm}^3$  and a molecular weight of  $81.4$   
140  $\text{g/mol}$ ,
- 141 • stabilizer AR (fenyl- $\beta$ -naphthylamine): density  $1.16 \text{ g/cm}^3$ , molecular weight  
142  $219.3 \text{ g/mol}$ ,

- 143       • accelerator T (tetramethylthiuram disulfide): density 1.5 g/cm<sup>3</sup>, molecular  
144       weight 240 g/mol.

145   The glycerolysate with a number average molecular weight of about 902.4 g/mol and  
146   a hydroxyl number of about 186.5 mg KOH/g was used as a plasticizer. This  
147   component was produced at the Department of Polymer Technology, Gdańsk  
148   University of Technology.

## 149   **2.2. THE PREPARATION OF COMPOSITES**

150       Five different composite specimens were prepared. Four composite samples  
151   contained different lignin contents, namely, 5, 10, 20 and 40 phr, and were coded  
152   WLI5G, WLI10G, WLI20G and WLI40G, respectively. The reference sample without  
153   lignin was also prepared (WLI0G). Before mixing, the natural rubber was annealed in  
154   air to improve the mastication process. The natural rubber was subjected to the  
155   mixing process in a BUZULUK open-roll machine (Datta and Głowińska, 2011). Then  
156   the ingredients were added in the quantities shown in Table 1. The friction ratio  
157   between the two rolls was about 1.1:1. All composites were vulcanized at a  
158   temperature of 146 °C with the use of hydraulic press produced by ZUP Nysa. The  
159   applied pressure was ca. 5 MPa. The vulcanization temperature was chosen in  
160   accordance with the reports by Jacob et. al. (Jacob et al., 2004) and Chonkaew et. al.  
161   (Chonkaew et al., 2010).

162

163   **Table 1** Composition of lignin-filled natural rubber-based composites.

164

## 165   **2.3. CHARACTERIZATION OF THE COMPOSITES**

166 Fourier Transform Infrared Spectroscopy was used to obtain the spectra of the  
167 samples of five composites, pure lignin, natural rubber, and glycerolysate. The  
168 measurements were carried out using a Nicolet 8700 FTIR spectrometer (Thermo  
169 Electron Corporation) with the use of ATR technique. The resolution was 4 cm<sup>-1</sup>.  
170 Sixty-four scans in the wavenumber range from 4500 to 500 cm<sup>-1</sup> were taken.

171 Scanning Electron Microscopy was used to characterize the cross-section  
172 morphology of the composites. The study was performed with the use of a Phenom  
173 G2 PRO scanning electron microscope (Phenom-World corporation) at the  
174 accelerating voltage of ca. 5 kV.

175 Dynamic mechanical tests were carried out with the use of a DMA Q 800  
176 analyzer (TA Instruments). The measurements were performed in accordance with  
177 ISO 6721-1, which allowed to obtain the values of storage modulus and tangent delta  
178 (damping factor) curves. The specimens with dimensions 30 x 5 x 2 mm were  
179 analyzed at a heating rate of ca. 4 °C/min for the temperature range from -100 to  
180 150°C. The tests were performed in air, with a frequency of 1 Hz.

181 Thermogravimetric analysis allowed to characterize the thermal stability of the  
182 prepared composites. The measurements were carried out with the use of a  
183 NETZSCH TG 209F3 analyzer. The specimens weighing ca. 5 mg each were  
184 analyzed under nitrogen atmosphere. The temperature used ranged from 35 to  
185 600°C at a heating rate of 20 °C/min.

186 The mechanical properties, such as tensile strength, elongation at break, and  
187 permanent elongation after break, were determined with the use of a Zwick/Roell  
188 Z020 universal testing machine. The tests were performed in accordance with ISO  
189 37, with the crosshead speed set to 300 mm/min and the 20 kN load cell. The



190 dumbbell-shaped specimens of all composites were tested. The obtained results are  
191 reported as average values calculated from three samples.

192 The hardness measurements were performed with a Shore type A Durometer  
193 (Zwick/Roell). The circular specimens with a thickness of 6 mm were tested in  
194 accordance with the standard ISO 868. The presented results are the mean values of  
195 hardness based on ten independent measurements.

196 A Schob machine was used to analyze the rebound resilience of the obtained  
197 materials. Tests were performed on the circular, 6-mm thick samples in accordance  
198 with ISO 4662. The mean values calculated from ten measurements are reported for  
199 all the composites.

200 The density of the produced materials was determined by using an electronic  
201 analytical balance equipped with a kit for measuring the density of solids. During the  
202 single test the sample was weighed in air and in the liquid of known density, namely,  
203 methanol with a density of ca. 0.790 g/cm<sup>3</sup>. All measurements were performed at a  
204 temperature of 23°C in accordance with ISO 2781. The presented results are the  
205 mean values calculated from three independent measurements.

206 The abrasion resistance was investigated with the use of a Schopper-  
207 Schlobbach instrument. All specimens were circles of diameter 17 mm. Tests were  
208 performed on three samples of each material in accordance with ISO 4649. The  
209 average values were calculated from three independent measurements. The  
210 abrasiveness  $V$  (cm<sup>3</sup>) was defined as a volume loss, and determined from equation  
211 (1):

212

213  $V = (m_0 - m_1) * m_t / (\rho * \Delta m_w)$  (1)

214

215 where:  $m_0$  (g) and  $m_1$  (g) are the sample mass before and after the test, respectively;  
216  $m_t$  (g) is a theoretical loss of weight of the reference mixture (assumed value of 0.2  
217 g);  $\rho$  (g/cm<sup>3</sup>) is the density of tested sample; and  $\Delta m_w$  (g) is the average weight loss  
218 of reference mixture with the known abrasiveness (assumed value of 0.1095 g).

219 The swelling parameters, such as swelling index, volume fraction of rubber  
220 network, molecular weight between crosslinks, and the crosslink density, were  
221 determined by employing the equilibrium swelling method. The tests were carried out  
222 according to the descriptions presented in the literature (Abdelmouleh et al., 2007;  
223 Bahl et al., 2014; Gregorová et al., 2006; Kosikova et al., 2007). The rectangular  
224 specimens with the average dimensions 15 x 15 x 2 mm were immersed in pure  
225 toluene (purchased from POCH, Gliwice, Poland). The measurements were carried  
226 out at room temperature for 7 days (168 hours). In this time period, samples were  
227 taken out from the immersion liquid to determine the weight change. The samples  
228 were dried on paper for one minute in air, then weighted and placed again in toluene.  
229 After obtaining the equilibrium swelling state, the samples were dried in air for 7 days  
230 and then subjected to annealing at a temperature of 80°C for 3 hours (Riyajan, 2015;  
231 Stelescu et al., 2014). The swelling ratio was calculated according to the following  
232 equation (2):

233

234  $SR = (m_a - m_b) / m_b * 100 \%$  (2)

235

236 where:  $m_b(g)$  and  $m_a(g)$  are the mean weights of analyzed samples before and after  
 237 swelling in the immersion liquid, respectively. In the next step of the procedure, the  
 238 volume fraction of rubber network,  $V_{fr}(-)$ , was calculated from equation (3):

239

$$240 \quad V_{fr} = V_r / (V_r + V_s) = (m_r/\rho_{rr}) / (m_r/\rho_{rr} + m_s/\rho_s) \quad (3)$$

241

242 where:  $V_r (cm^3)$  and  $V_s (cm^3)$  are the mean volumes of rubber and solvent in the  
 243 swollen sample, respectively;  $m_r(g)$  and  $m_s (g)$  are the mean weights of rubber and  
 244 solvent in the analyzed samples after swelling in the immersion liquid, respectively;  
 245  $\rho_{rr}(g/cm^3)$  and  $\rho_s (g/cm^3)$  are the respective densities of rubber (0.9125 g/cm<sup>3</sup> for  
 246 natural rubber) and solvent (0.867 g/cm<sup>3</sup> for toluene) in the composites.

247 The average molecular weight between crosslinks,  $M_c (g/mol)$  was determined  
 248 by using the Flory–Rehner theory according to the following equation (4):

249

$$250 \quad M_c = \frac{-\rho_r \times V_s \times \left( V_{fr}^{\frac{1}{3}} - \frac{1}{2} V_{fr} \right)}{\ln(1 - V_{fr}) + V_{fr} + (\chi \times V_{fr}^2)} \quad (4)$$

251

252 where:  $\rho_r(g/cm^3)$  means the density of lignin-rubber composites;  $V_s$  is the molar  
 253 volume of solvent (106.52 cm<sup>3</sup>/mol for toluene); and  $\chi$  is the Huggins parameter,  
 254 defining the interaction between the polymer and solvent (0.38 for natural rubber-  
 255 toluene).

256 The crosslink density,  $v$  (mol/cm<sup>3</sup>), was determined from equation (5):

257

$$258 \quad v = \rho_r / M_c \quad (5)$$

259

260 where:  $\rho_r$ (g/cm<sup>3</sup>) means the polymer density (lignin-rubber composite), and  $M_c$   
261 (g/mol) is the average molecular weight of polymer.

## 262 **3. RESULTS AND DISCUSSION**

### 263 **3.1. FOURIER TRANSFORM INFRARED (FTIR) SPECTROSCOPY**

264 Fourier Transform Infrared analysis was used to investigate the chemical  
265 structure of the prepared lignin/rubber composites, pure lignin, natural rubber and  
266 glycerolysate used. The FTIR spectra of all composite samples (Figure 1a)  
267 demonstrated similar profiles.

268

269 **Figure 1** a) FTIR spectra of the composites, pure lignin, natural rubber and  
270 glycerolysate; b) FTIR spectra of the obtained specimens for the wavenumbers  
271 ranging from 1800 to 800 cm<sup>-1</sup>.

272

273 More differences were associated with the varying intensity of characteristic  
274 peaks. For the samples without the natural rubber, the characteristic wide vibration  
275 was present in all spectra in the wavelength range between 3570 and 3170 cm<sup>-1</sup>,  
276 which was attributable to the stretching vibrations of hydroxyl groups derived from



277 lignin and glycerolysate (Kubačková et al., 2013). The strong peaks with the highest  
278 intensity at 2960, 2918 and 2850  $\text{cm}^{-1}$  correspond to the stretching vibrations of the  
279  $\text{CH}_3$ ,  $\text{CH}_2$ ,  $\text{CH}$  groups from cis-1,4-polyisoprene macromolecules and glycerolysate  
280 (Riyajan, 2015) , however, the lignin particles also revealed a small shift in this  
281 wavenumber range.

282 For a better visibility, the FTIR spectra of samples in the wavelength range  
283 from 1800 to 800  $\text{cm}^{-1}$  were presented in Figure 1 b. The intensive peak at 1596  $\text{cm}^{-1}$   
284 is attributable to the symmetric aromatic skeletal vibration indicated by lignin  
285 macromolecules (Faruket al., 2016c). Other strong bands at 1515  $\text{cm}^{-1}$  are related to  
286 the asymmetric aryl ring stretching corresponding to lignin (Faruket al., 2016c). The  
287 absorption at ca. 1445  $\text{cm}^{-1}$  was assigned to the deformation vibrations of methyl  
288 groups  $-\text{CH}$  is related to the lignin aromatic rings, and also to the natural rubber  
289 chains (Joseph et al., 2010). The band near 1377  $\text{cm}^{-1}$  is attributable to the  
290 asymmetric vibrations of the methyl  $-\text{CH}$  groups derived from the natural rubber  
291 chain as well as glycerolysate (Datta and Włoch, 2015). The absorption at ca. 1266  
292  $\text{cm}^{-1}$  was assigned to the stretching vibrations of the  $-\text{C}-\text{O}$  groups present in the  
293 phenolic rings of lignin. The peaks at ca. 1127 and 1030  $\text{cm}^{-1}$  were attributed to the  
294 aromatic  $-\text{CH}$  groups in-plane deformation stretching originating from lignin (Faruket  
295 al., 2016c). In the case of glycerolysate, the most intensive peak at a wavenumber of  
296 1094  $\text{cm}^{-1}$  was attributable to the stretching vibration of the  $\text{C}-\text{O}$  group. The peak  
297 near the wavelength of ca. 839  $\text{cm}^{-1}$  was related to the variations of  $-\text{CH}$  groups in  
298 the rubber chains (Lin et al., 2015).

299 It is noteworthy that the intensity of characteristic peaks did not increase with  
300 the increasing amount of lignin in the composites. That can be explained by the

301 formation of lignin agglomerates, which occurs as the amount of lignin increases. The  
302 accumulation of lignin particles results in the disturbance of the spectrum.

303 The interaction between the lignin units and the natural rubber chain can be  
304 explained based on the FTIR results. Jiang et al. (Jianget al., 2013) described the  
305 interaction between lignin and the poly(diallyldimethylammonium chloride)  
306 (PDADMAC) chain by comparing the shifts in the FTIR peaks corresponding to the  
307 stretching vibration of the -CH groups due to the presence of double bonds. The  
308 authors also indicated that lignin interacts with the rubber chains in the same way  
309 because of the similarity between the chain skeletons of NR and PDADMAC. In  
310 Figure 1 b, the peaks at 1515 and 1596  $\text{cm}^{-1}$  in the spectrum of pure lignin shift to the  
311 respective locations at 1545 and 1600  $\text{cm}^{-1}$  in the spectra of composites. A small shift  
312 from a wavenumber of 1445  $\text{cm}^{-1}$  to 1450  $\text{cm}^{-1}$  is also visible, which is associated with  
313 the vibration of the natural rubber chain. This little shift indicates a noncovalent  
314 interaction between the NR chain and lignin due to the adsorption of NR onto lignin.  
315 The similar results were presented by Pillai and Rennekar(Pillaiand Rennekar,  
316 2009) , and Yang and co-workers (Yanget al., 2005).

### 317 **3.2. SCANNING ELECTRON MICROSCOPY (SEM)**

318 The cross-sections of specimens were assessed by the scanning electron  
319 microscopy in order to characterize the lignin dispersion in the composites. In  
320 addition, the SEM micrographs revealed the interaction between the lignin powder  
321 and the natural rubber matrix. Figures 2a and 2b show the specimens without lignin  
322 and those containing 5 phr of lignin, respectively. It has been demonstrated that the  
323 dispersion of this lowest quantity of lignin was satisfactory, without any visible  
324 agglomerates. Other specimens, i.e. WLI10G, WLI20G and WLI40G showed the

325 accumulation of lignin particles. The lignin agglomerates were of irregular shape with  
326 approximate dimensions from several to several tens of micrometers (Jianget al.,  
327 2015). This finding explains the formation of hydrogen bonds between the lignin  
328 particles. It also indicates that the aggregation of lignin is unavoidable in the natural  
329 rubber matrix without additional modifications (Jianget al., 2013). Moreover, it is well  
330 known that the composites with highly dispersed filler in the rubber can bear higher  
331 stress in comparison to the composites containing the filler agglomerates. The  
332 concentration of lignin particles in the obtained composites results in a decrease in  
333 resistance (Jianget al., 2015). It is noteworthy that the observed agglomerates did not  
334 expand with increasing lignin content in the composites, however, their number  
335 increased. This can be explained by the glycerolysate content, which can suppress  
336 the accumulation of lignin particles into larger agglomerates despite the lignin  
337 polydispersity, and its propensity to form larger agglomerates with increasing lignin  
338 concentration.

339

340 **Figure 2** SEM images of a) reference samples, WLI0G; b) samples containing 5 phr  
341 of lignin, WLI5G; c) samples with 10 phr of lignin, WLI10G; d) samples with 20 phr of  
342 lignin, WLI20G; and e) samples with 40 phr of lignin, WLI40G.

343

### 344 **3.3. DYNAMIC MECHANICAL ANALYSIS (DMA)**

345 The dynamic mechanical behavior of the lignin-rubber composites was  
346 investigated with the use of dynamic mechanical analysis. The variation of the  
347 storage modulus logarithm,  $\log E'$  versus temperature, and variation of tangent delta,  
348  $\tan \delta$  versus temperature were determined (Figures 3 and 4).



349

350 **Figure 3** The logarithm of storage modulus (Log E') of the lignin-rubber composites  
351 plotted versus temperature.

352

353 The characteristics of the Log E' vs. temperature curve are typical for thermoplastic  
354 polymers with high molecular weights. The relationship between the storage modulus  
355 and temperature for the temperature range from -100 to ca. -50°C was linear. The  
356 underlying cause of this behavior is the presence of natural rubber which, at the  
357 aforementioned temperature range, occurs is the glassy state, and does not generate  
358 the reinforcing effect with the filler (Braset al., 2010). After achieving the temperature  
359 of ca. -50°C, a sharp decreasing trend was observed in the curve. This phenomenon  
360 is related to the alfa transition temperature of the natural rubber matrix. The midpoint  
361 of the decreasing curve at the temperature range from ca. -50 to ca. 0°C indicates  
362 the position of the glass transition temperature,  $T_g$ (Chonkaew et al., 2010;  
363 Geethamma et al., 2005). This point is closely associated with the relaxation of the  
364 long chain sequences of natural rubber. Cooperative motion of macromolecules  
365 induce the dissipation of energy at the temperature of maximum  $\tan \delta$  (Figure 4)  
366 (Abdelmouleh et al., 2007). The curve characteristics at around 0°C are related to the  
367 melting of the remaining crystalline regions in the macromolecule matrix (Gopalan  
368 Nair and Dufresne, 2003).

369

370 **Figure 4** Tan  $\delta$  as a function of temperature of the lignin-rubber composites.

371



372 The addition of the various amounts of lignin to the composites resulted in a  
373 decrease in the alfa transition temperature. The lowest value, i.e. ca. -44 °C was  
374 determined for the specimens containing 10 and 40 phr of lignin (Table 2). These  
375 results can be explained by impaired chain mobility due to the lignin addition, which is  
376 an obstacle for generating significant reinforcement in the composite (Chonkaew et  
377 al., 2010). The highest  $\tan \delta$  peak was observed in the reference sample. With  
378 increasing lignin content, the peak intensity decreased. Because the filler particles  
379 were surrounded by the rubber matrix and the hydrogen bonds formed, the  
380 movement of macromolecule chains was reduced, which resulted in the decreased  
381 intensity of the peaks (Kargarzadeh et al., 2015).

382

383 **Table 2** Alfa transition temperature [°C] of the lignin-rubber composites.

384

### 385 **3.4. THERMOGRAVIMETRIC ANALYSIS (TGA)**

386 The thermal stability of the composites, reference sample and pure lignin was  
387 investigated with the use of thermogravimetric analysis. The measurements allowed  
388 for plotting the thermogravimetric (TGA; Figure 5) and differential thermogravimetric  
389 (DTG; Figure 6) graphs.

390

391 **Figure 5** Thermogravimetric (TGA) curves for pure lignin, reference samples, and  
392 lignin-rubber composites with different lignin content.

393

394 **Figure 6** Differential thermogravimetric (DTG) curves for pure lignin, reference  
395 samples, and lignin-rubber composites with different lignin content.

396

397 Both aforementioned figures present one step of thermal decomposition for all  
398 samples. The highest rate of weight loss was observed in the sample of pure lignin.  
399 The samples of lignin-rubber composites showed an increase in the weight loss rate  
400 with increasing lignin content. In comparison to the reference sample, the composites  
401 containing higher lignin levels lost weight at the lower temperature (a 5% weight loss  
402 temperature). This was caused by the effect of lignin on the thermal properties of the  
403 prepared composites. Despite the aforementioned finding, the maximum rate of mass  
404 loss for all the composites occurred at the same temperature (390°C), except for the  
405 reference sample and pure lignin. For the latter two, the maximum rate of weight loss  
406 was observed at the lower temperature. In the case of temperatures of 50% and 80%  
407 weight loss, the samples displayed a similar range of maximum rate. Table 3  
408 presents the thermal degradation characteristics for all the analyzed samples.

409

410 **Table 3** Thermal degradation characteristics of the lignin-rubber composites and pure  
411 lignin, where  $T_{5\%}$  is a temperature of 5% weight loss,  $T_{50\%}$  is a temperature of 50%  
412 weight loss,  $T_{80\%}$  is a temperature of 80% weight loss, and  $T_{\max}$  is a temperature of  
413 the maximum rate of weight loss. Residue at 600°C [%].

414

415 The residual weight after TGA analysis (at 600°C) increased with increasing  
416 lignin content. This resulted from the presence of the highest lignin content. The

417 residue at 600°C comprised of ash, which consisted of organic and inorganic  
418 impurities. The impurities play an important role because they influence the thermal  
419 properties of lignin. The content of contaminants reduced the possibility of lignin  
420 softening in the composites, and decreased the quality of the filler. Moreover, due to  
421 the presence of impurities, thermal motion is hindered thereby preventing the thermal  
422 processing (Hu,2002; Kadla et al., 2002).

### 423 **3.5. MECHANICAL PROPERTIES**

424 The mechanical properties of the composites, such as tensile strength,  
425 elongation at break, and permanent elongation after break, were investigated. In  
426 order to characterize the prepared materials, their hardness, rebound resilience,  
427 density and abrasiveness were measured. Figure 7 shows the effect of varying  
428 amounts of lignin on the tensile strength of the composites.

429

430 **Figure 7** Stress-strain curve of the rubber composites.

431

432 It was found that the tensile properties of the samples decreased with  
433 increasing lignin content. The composites with a low amount of filler (WLI5G and  
434 WLI10G) showed a decrease in the elongation at break and tensile strength. The  
435 specimens containing 10 phr of lignin displayed the characteristics which were similar  
436 to those of the reference sample, however, they had lower tensile strength. In the  
437 case of the samples containing 20 and 40 phr lignin, they were characterized by the  
438 higher (WLI20G) or similar (WLI40G) elongation at break, and lower tensile strength  
439 than the reference sample. The lignin admixture in the composites caused a

440 decrease in the deformation resistance of rubber chains. Yu et al. (Yu et al., 2015)  
441 obtained similar results. Table 4 presents the results of tensile measurements.

442

443 **Table 4** The effect of lignin content on the tensile properties of lignin/natural rubber  
444 composites.

445

446 The interaction between the rubber chain and the filler particles hindered the  
447 return of macromolecules to the pre-test state. For this reason, the lignin rubber  
448 composites showed an increase in the permanent elongation after break. The  
449 specimen containing 5 phr of lignin was an exception because its permanent  
450 elongation decreased.

451 In Table 5 the results of hardness, resilience, density and abrasiveness  
452 measurements are presented.

453

454 **Table 5** The results of hardness, resilience, density and abrasiveness tests for the  
455 analyzed composites.

456

457 For the samples with 5 and 10 phr of lignin added, hardness of the analyzed  
458 composites slightly increased. In the case of the remaining filled samples, the  
459 hardness values decreased. It is known that the hardness of composites is closely  
460 related to the crosslink density (Stelescu et al., 2014). The maximum hardness at ca.  
461 45 °Sh A was measured in the sample containing 5 phr of lignin. A decrease in

462 hardness with increasing lignin content was correlated with the reduced crosslink  
463 density. The differences were observed in the case of the composite samples  
464 containing 5 phr of lignin. Those samples were characterized by higher hardness  
465 than the reference sample and other specimens. Thereby, the crosslink density of  
466 this particular composite displayed the greatest value.

467 Rebound resilience is also correlated with the crosslink density of composites.  
468 It was clearly demonstrated in this study that with increasing lignin content the  
469 crosslink density decreased (except for WLI5G), and thus the elasticity was also  
470 reduced which led to more rigid composites. Stelescu et al. obtained similar results  
471 (Stelescu et al., 2010).

472 Density is strictly related to the lignin amount, therefore, the highest density  
473 was measured in sample WLI40G, while the lowest, in WLI0G.

474 The composite with a 5 phr of lignin admixture showed the lowest  
475 abrasiveness compared to the remaining composites. This finding is clearly  
476 connected to the crosslink density of this specimen, which was the highest. For the  
477 remaining composites, the abrasion resistance decreased with increasing lignin  
478 content.

### 479 **3.6. EQUILIBRIUM SWELLING PROPERTIES**

480 The effect of lignin content on the composite network structures was  
481 investigated via the equilibrium swelling test. The following parameters were  
482 determined: the volume fraction of rubber, molecular weight between the crosslinks,  
483 crosslink density, and swelling ratio all of composites. Table 6 presents the results of  
484 those measurements.

485

486 **Table 6** The results of equilibrium swelling measurements performed on the lignin-  
487 rubber composites.

488

489 With increasing lignin content the swelling ratio of the composites decreased  
490 (Table 6) in comparison to the reference specimen. The swelling ratio increased only  
491 in the case of the composites with the highest lignin content. M. Jacob et al. (Jacobet  
492 al., 2004) pointed out that the solvent diffusion mechanism in the rubber matrix is  
493 correlated with the polymer's ability to form voids suitable for the solvent uptake. With  
494 increasing lignin content in the composites, the number of voids in the rubber matrix  
495 decreased, locking the pathways for the solvent, and thus the solvent uptake also  
496 decreased. The highest value of the swelling ratio of the specimen with a 40 phr  
497 lignin content is related to the most numerous formation of agglomerates with the  
498 highest volume. The aforementioned amount of lignin in the composite is too high for  
499 the successful hydrogen bond formation between the lignin particles and the natural  
500 rubber matrix. As a result, the lignin particles can leach out from the samples during  
501 the swelling ratio measurements, which makes the high solvent uptake possible. The  
502 swelling ratio is related to the crosslink density. (Jacobet al., 2004; Park and Cho,  
503 2003) suggested that the maximum interaction between the rubber chain and filler,  
504 and the lowest crosslink density are characteristic for the composites with the highest  
505 admixture of lignin. The obtained results showed that the lignin content caused a  
506 decrease in the crosslink density (Table 6). Lignin in the natural rubber vulcanizates  
507 lowers the number of polysulfidic crosslinks between the rubber chains if the disulfidic  
508 and monosulfidic crosslinks remain constant (Faruket al., 2016b). The decreased



509 amount of polysulfides lowers the hardness, resilience, abrasion resistance and  
510 tensile properties (Stelescu et al., 2010). The lignin particles mask some of the sites  
511 on the natural rubber molecules, that otherwise would have been available for  
512 crosslinking (Kumaran et al., 1978) , and cause a decrease in the network density.  
513 Due to the occurrence of masked crosslinking sites, the distance between the  
514 network nodes increases. The larger distance between the networks leads to the  
515 polymer chain tangling. The increased molecular weight between crosslinks (see  
516 Table 6) is a proof of the increased complexity of natural rubber macromolecules  
517 between the network nodes.

518 During the equilibrium swelling measurements the values of weight loss were  
519 recorded over time (Figure 8). The samples containing 5 and 10 phr of lignin  
520 displayed a lower weight change than the reference samples. The sample with a 5  
521 phr lignin content showed the lowest weight loss. The two composites with the  
522 highest lignin contents displayed a higher weight loss than the reference samples.  
523 The performed measurement allowed for concluding that a low lignin content in the  
524 composites containing glycerolysate as a plasticizer, resulted in a decrease in the  
525 solvent (toluene) absorption.

526

527 **Figure 8** Weight loss during the swelling measurements performed on the lignin-  
528 rubber composites.

529

#### 530 4. CONCLUSIONS

531 The softwood-lignin/natural rubber composites were successfully prepared  
532 with the use of a novel plasticizer. Nowadays, the plasticizers mainly originate from  
533 the petrochemical resources. Glycerolysate used in this work is the product of the  
534 chemical recycling of polyurethanes. The results of the presented research  
535 demonstrated that the mechanical and thermal properties of softwood-lignin/natural  
536 rubber composites obtained with the use of glycerolysate as a plasticizer are similar  
537 to those of the lignin-containing composites prepared with other commercially  
538 available plasticizing agents. In addition, the data showed that the composite  
539 containing 5 phr of lignin displayed the best properties. Specimen WLI5G had the  
540 highest values of hardness and abrasiveness, and superior tensile properties. The  
541 Scanning Electron Microscopy (SEM) confirmed a positive interaction between the  
542 rubber chains and the lignin particles. The SEM images of composite WLI5G showed  
543 good dispersion of lignin, without the lignin agglomerates. The prepared four  
544 composite formulas with increasing lignin content allowed the determination of  
545 maximum lignin content in the composite that would not alter the material's positive  
546 properties. The composite containing the highest amount of lignin (WLI40G) had the  
547 biggest and most numerous agglomerates and, consequently, the worst mechanical  
548 (the lowest values of tensile strength, elongation after break, etc.) and thermal  
549 properties (e.g. the fastest weight loss). This observation has been confirmed by the  
550 results of swelling measurements, where sample WLI40G displayed the highest  
551 swelling ratio. The application of lignin that is the product of natural origin, and the  
552 use of the product of the chemical recycling of polyurethanes makes the described  
553 procedure eco-friendly. Its economic advantages should also be considered.  
554 Glycerolysate, used as a plasticizing agent, is less expensive than the commonly  
555 employed plasticizers derived from petrochemicals. In summary, this work is a





556 promising development in the field of natural product utilization, and the application of  
557 the products of chemical recycling in the natural rubber matrix.

#### 558 ACKNOWLEDGMENTS

559 The authors gratefully acknowledge receiving the samples of lignin powder  
560 used in this study from MeadWestvaco Corporation, Specialty Chemical Division,  
561 South Carolina (USA).

562

563

564 REFERENCES:

- 565 Abdelmouleh, M., Boufi, S., Belgacem, M.N., Dufresne, A., 2007. Short natural-fibre  
566 reinforced polyethylene and natural rubber composites: Effect of silane coupling  
567 agents and fibres loading. *Compos. Sci. Technol.* 67, 1627–1639.  
568 doi:10.1016/j.compscitech.2006.07.003
- 569 Alexander, M., Thachil, E.T., 2006. A comparative study of cardanol and aromatic oil  
570 as plasticizers for carbon-black-filled natural rubber. *J. Appl. Polym. Sci.* 102,  
571 4835–4841. doi:10.1002/app.24811
- 572 Altenhofen Da Silva, M., Adeodato Vieira, M.G., Gomes Maumoto, A.C., Beppu,  
573 M.M., 2011. Polyvinylchloride (PVC) and natural rubber films plasticized with a  
574 natural polymeric plasticizer obtained through polyesterification of rice fatty acid.  
575 *Polym. Test.* 30, 478–484. doi:10.1016/j.polymertesting.2011.03.008
- 576 Bahl, K., Swanson, N., Pugh, C., Jana, S.C., 2014. Polybutadiene-g-  
577 poly(pentafluorostyrene) as a coupling agent for lignin-filled rubber compounds.  
578 *Polymer (Guildf)*. 55, 6754–6763. doi:10.1016/j.polymer.2014.11.008
- 579 Bjornsson, S., 2014. *Advanced Control Methodology for Biomass Combustion*.  
580 University of Washington.
- 581 Bras, J., Hassan, M.L., Bruzesse, C., Hassan, E.A., El-Wakil, N.A., Dufresne, A.,  
582 2010. Mechanical, barrier, and biodegradability properties of bagasse cellulose  
583 whiskers reinforced natural rubber nanocomposites. *Ind. Crops Prod.* 32, 627–  
584 633. doi:10.1016/j.indcrop.2010.07.018
- 585 Chakar, F.S., Ragauskas, A.J., 2004. Review of current and future softwood kraft  
586 lignin process chemistry. *Ind. Crops Prod.* 20, 131–141.

- 587 doi:10.1016/j.indcrop.2004.04.016
- 588 Chonkaew, W., Minghvanish, W., Kungliyan, U., Rochanawipart, N., Brostow, W.,  
589 2010. Vulcanization characteristics and dynamic mechanical behavior of natural  
590 rubber reinforced with silane modified silica. *J. Nanosci. Nanotechnol.* 10, 2018–  
591 2024. doi:10.1166/jnn.2011.3563
- 592 Datta, J., 2010. Synthesis and Investigation of Glycolysates and Obtained  
593 Polyurethane Elastomers. *J. Elastomers Plast.* 42, 117–127.  
594 doi:10.1177/0095244309354368
- 595 Datta, J., Głowińska, E., 2011. Influence of cellulose on mechanical and  
596 thermomechanical properties of elastomers obtained from mixtures containing  
597 natural rubber. *Polimery* 61, 823–827.
- 598 Datta, J., Pasternak, S., 2005. Oligourethane glycols obtained in glycolysis of  
599 polyurethane foam as semi-finished products for cast urethane elastomers  
600 preparation. *Polimery* 50, 352–357.
- 601 Datta, J., Włoch, M., 2015. Morphology and properties of recycled  
602 polyethylene/ground tyre rubber/thermoplastic poly(ester-urethane) blends.  
603 *Macromol. Res.* 23, 1–10. doi:10.1007/s13233-015-3155-5
- 604 De Wild, P.J., Huijgen, W.J.J., Gosselink, R.J.A., 2014. Lignin pyrolysis for profitable  
605 lignocellulosic biorefineries. *Biofuels, Bioprod. Biorefining* 8, 645–657.  
606 doi:10.1002/bbb.1474
- 607 Faruk, O., Sain, M., Haghdan, S., Renneckar, S., Smith, G.D., 2016a. Lignin in  
608 Polymer Composites, *Lignin in Polymer Composites*. Elsevier.  
609 doi:10.1016/B978-0-323-35565-0.00001-1



- 610 Faruk, O., Sain, M., Kakroodi, A.R., 2016b. Lignin in Polymer Composites, Lignin in  
611 Polymer Composites. Elsevier. doi:10.1016/B978-0-323-35565-0.00010-2
- 612 Faruk, O., Sain, M., Stark, N.M., Yelle, D.J., Agarwal, U.P., 2016c. Lignin in Polymer  
613 Composites, Lignin in Polymer Composites. Elsevier. doi:10.1016/B978-0-323-  
614 35565-0.00004-7
- 615 Geethamma, V.G., Kalaprasad, G., Groeninckx, G., Thomas, S., 2005. Dynamic  
616 mechanical behavior of short coir fiber reinforced natural rubber composites.  
617 Compos. Part A Appl. Sci. Manuf. 36, 1499–1506.  
618 doi:10.1016/j.compositesa.2005.03.004
- 619 Gopalan Nair, K., Dufresne, A., 2003. Crab shell chitin whisker reinforced natural  
620 rubber nanocomposites. 1. Processing and swelling behavior.  
621 Biomacromolecules 4, 657–665. doi:10.1021/bm020127b
- 622 Gregorová, A., Košíková, B., Moravčík, R., 2006. Stabilization effect of lignin in  
623 natural rubber. Polym. Degrad. Stab. 91, 229–233.  
624 doi:10.1016/j.polymdegradstab.2005.05.009
- 625 Hatakeyama, H., Hatakeyama, T., 2010. Biopolymers: Lignin, Proteins, Bioactive  
626 Nanocomposites, in: Abe, A., Dusek, K., Kobayashi, S. (Eds.), . Springer Berlin  
627 Heidelberg, Berlin. doi:10.1007/12\_2009\_12
- 628 Holladay, J.E., White, J.F., Bozell, J.J., Johnson, D., 2007. Top Value-Added  
629 Chemicals from Biomass - Volume II?Results of Screening for Potential  
630 Candidates from Biorefinery Lignin. Evaluation II, 87. doi:10.2172/921839
- 631 Hu, T.Q., 2002. Chemical modification, properties and usage of lignin, Spronger  
632 Science and Business Media. doi:10.1017/CBO9781107415324.004

- 633 Jacob, M., Thomas, S., Varughese, K.T., 2004. Mechanical properties of sisal/oil  
634 palm hybrid fiber reinforced natural rubber composites. *Compos. Sci. Technol.*  
635 64, 955–965. doi:10.1016/S0266-3538(03)00261-6
- 636 Jiang, C., He, H., Jiang, H., Ma, L., Jia, D.M., 2013. Nano-lignin filled natural rubber  
637 composites: Preparation and characterization. *eXPRESSPolym. Lett.* 5, 480–  
638 493.
- 639 Jiang, C., He, H., Yao, X., Yu, P., Zhou, L., Jia, D., 2015. In situ dispersion and  
640 compatibilization of lignin/epoxidized natural rubber composites: reactivity,  
641 morphology and property. *J. Appl. Polym. Sci.* 132, 1–10.  
642 doi:10.1002/app.42044
- 643 Jiang, C., He, H., Yao, X., Yu, P., Zhou, L., Jia, D., 2014. Self-crosslinkable  
644 lignin/epoxidized natural rubber composites. *J. Appl. Polym. Sci.* 131, 1–9.  
645 doi:10.1002/app.41166
- 646 Joseph, S., Appukuttan, S.P., Kenny, J.M., Puglia, D., Thomas, S., Joseph, K., 2010.  
647 Dynamic Mechanical Properties of Oil Palm Microfibril-Reinforced Natural  
648 Rubber Composites. *Polymer (Guildf)*. 117, 1298–1308. doi:10.1002/app
- 649 Kadla, J.F., Kubo, S., Venditti, R.A., Gilbert, R.D., Compere, A.L., Griffith, W., 2002.  
650 Lignin-based carbon fibers for composite fiber applications. *Carbon N. Y.* 40,  
651 2913–2920. doi:10.1016/S0008-6223(02)00248-8
- 652 Kargarzadeh, H., Sheltami, R.M., Ahmad, I., Abdullah, I., Dufresne, A., 2015.  
653 Cellulose nanocrystal reinforced liquid natural rubber toughened unsaturated  
654 polyester: Effects of filler content and surface treatment on its morphological,  
655 thermal, mechanical, and viscoelastic properties. *Polymer (Guildf)*. 71, 51–59.

- 656 doi:10.1016/j.polymer.2015.06.045
- 657 Kopczyńska, P., Datta, J., 2016. Single-phase product obtained via crude glycerine  
658 depolymerisation of polyurethane elastomer: Structure characterisation and  
659 rheological behaviour. *Polym. Int.* doi:10.1002/pi.5128
- 660 Kosikova, B., Gregorova, A., Osvald, A., Krajcovicova, J., 2007. Role of Lignin Filler  
661 in Stabilization of Natural Rubber – Based Composites. *J. Appl. Polym. Sci.* 103,  
662 1226–1231. doi:10.1002/app
- 663 Kubačková, J., Ferenc, J., Hudec, I., Šutý, Š., Jablonský, M., Annus, J., Pret'o, J.,  
664 2013. Antioxidant properties of lignin in rubber blends. *Elastomery* 17, 21–27.
- 665 Kumaran, M.G., Mukhopadhyay, R., De, S.K., 1978. Effect of accelerator system and  
666 addition of lignin on the network structure of natural rubber vulcanizate. *Polymer*  
667 (Guildf). 19, 461–463. doi:10.1016/0032-3861(78)90258-6
- 668 Lin, Y., Chen, Y., Zeng, Z., Zhu, J., Wei, Y., Li, F., Liu, L., 2015. Effect of ZnO  
669 nanoparticles doped graphene on static and dynamic mechanical properties of  
670 natural rubber composites. *Compos. Part A* 70, 35–44.  
671 doi:10.1016/j.compositesa.2014.12.008
- 672 Mohapatra, S., Nando, G.B., 2014. Cardanol: a green substitute for aromatic oil as a  
673 plasticizer in natural rubber. *Rsc Adv.* 4, 15406–15418. doi:Doi  
674 10.1039/C3ra46061d
- 675 Neutelings, G., 2011. Lignin variability in plant cell walls: contribution of new models.  
676 *Plant Sci.* 181, 379–86. doi:10.1016/j.plantsci.2011.06.012
- 677 Nikje, M.M.A., Nikrah, M., 2007. Glycerin as a new glycolysing agent for chemical

- 678 recycling of cold cure polyurethane foam wastes in “split-phase” condition.  
679 Polym. Bull. 58, 411–423. doi:10.1007/s00289-006-0683-3
- 680 Park, S.J., Cho, K.S., 2003. Filler-elastomer interactions: Influence of silane coupling  
681 agent on crosslink density and thermal stability of silica/rubber composites. J.  
682 Colloid Interface Sci. 267, 86–91. doi:10.1016/S0021-9797(03)00132-2
- 683 Pillai, K. V., Rennekar, S., 2009. Cation- $\pi$  interactions as a mechanism in technical  
684 lignin adsorption to cationic surfaces. Biomacromolecules 10, 798–804.  
685 doi:10.1021/bm801284y
- 686 Riyajan, S.-A., 2015. Robust and biodegradable polymer of cassava starch and  
687 modified natural rubber. Carbohydr. Polym. 134, 267–277.  
688 doi:10.1016/j.carbpol.2015.07.038
- 689 Rogers, D., 2015. Lignin-Derived Thermosetting Vinyl Ester Resins for High  
690 Performance Applications.
- 691 Simon, D., Borreguero, A.M., De Lucas, A., Rodriguez, J.F., 2014. Glycolysis of  
692 flexible polyurethane wastes containing polymeric polyols. Polym. Degrad. Stab.  
693 109, 115–121. doi:10.1016/j.polymdegradstab.2014.07.009
- 694 Simón, D., de Lucas, A., Rodríguez, J.F., Borreguero, A.M., 2016. Glycolysis of high  
695 resilience flexible polyurethane foams containing polyurethane dispersion polyol.  
696 Polym. Degrad. Stab. 133. doi:10.1016/j.polymdegradstab.2016.08.007
- 697 Stelescu, M., Manaila, E., Craciun, G., Dumitrascu, M., 2014. New Green Polymeric  
698 Composites Based on Hemp and Natural Rubber Processed by Electron Beam  
699 Irradiation. Sci. World J. 2014, 1–13.

- 700 Stelescu, M.D., Georgescu, M., Manaila, E., 2010. Aspects Regarding Crosslinking of  
701 a Natural Rubber Blend, in: Proceedings of the 3rd International Conference on  
702 Advanced Materials and Systems. pp. 313–318.
- 703 Vieira, M.G.A., Da Silva, M.A., Dos Santos, L.O., Beppu, M.M., 2011. Natural-based  
704 plasticizers and biopolymer films: A review. Eur. Polym. J. 47, 254–263.  
705 doi:10.1016/j.eurpolymj.2010.12.011
- 706 Yang, D., Rochette, J., Sacher, E., 2005. Spectroscopic Evidence for  $\pi$ - $\pi$  Interaction  
707 between Poly ( diallyldimethylammonium ) Chloride and Multiwalled Carbon  
708 Nanotubes. J. Phys. Chem. B 109, 4481–4484.
- 709 Yu, P., He, H., Jiang, C., Wang, D., Jia, Y., Zhou, L., Jia, D.M., 2015. Reinforcing  
710 styrene butadiene rubber with lignin-novolac epoxy resin networks.  
711 eXPRESSPolym. Lett. 9, 36–48.



712 Figure Captions

713 **Figure 1** a) FTIR spectra of the composites, pure lignin, natural rubber and  
714 glycerolysate; b) FTIR spectra of the obtained specimens for the wavenumbers  
715 ranging from 1800 to 800  $\text{cm}^{-1}$ .

716 **Figure 2** SEM images of a) reference samples, WLI0G; b) samples containing 5 phr  
717 of lignin, WLI5G; c) samples with 10 phr of lignin, WLI10G; d) samples with 20 phr of  
718 lignin, WLI20G; and e) samples with 40 phr of lignin, WLI40G.

719 **Figure 3** The logarithm of storage modulus ( $\text{Log } E'$ ) of the lignin-rubber composites  
720 plotted versus temperature.

721 **Figure 4**  $\text{Tan } \delta$  as a function of temperature of the lignin-rubber composites.

722 **Figure 5** Thermogravimetric (TGA) curves for pure lignin, reference samples, and  
723 lignin-rubber composites with different lignin content.

724 **Figure 6** Differential thermogravimetric (DTG) curves for pure lignin, reference  
725 samples, and lignin-rubber composites with different lignin content.

726 **Figure 7** Stress-strain curve of the rubber composites.

727 **Figure 8** Weight loss during the swelling measurements performed on the lignin-  
728 rubber composites.

729 **Table 1** Composition of lignin filled natural rubber-based composites.

COMPONENT	QUANTITIES OF INGREDIENTS (phr)				
	WLI0G	WLI5G	WLI10G	WLI20G	WLI40G
Natural rubber	100	100	100	100	100
Stearic acid	3	3	3	3	3
Zinc oxide	5	5	5	5	5
Stabilizer AR	1.5	1.5	1.5	1.5	1.5
Accelerator T	0.5	0.5	0.5	0.5	0.5
Glycerolysate	2	2	2	2	2
Lignin (INDULIN AT)	0	5	10	20	40
Sulphur	3	3	3	3	3

730

731 **Table 2** Alfa transition temperature [°C] of the lignin-rubber composites.

Composite	Alfa transition temperature
	$T_{\alpha}$ [°C]
WLI0G	-38
WLI5G	-40
WLI10G	-44
WLI20G	-41
WLI40G	-43

732

733 **Table 3** Thermal degradation characteristics of the lignin-rubber composites and pure  
 734 lignin, where  $T_{5\%}$  is a temperature of 5% weight loss,  $T_{50\%}$  is a temperature of 50%  
 735 weight loss,  $T_{80\%}$  is a temperature of 80% weight loss, and  $T_{\max}$  is a temperature of  
 736 the maximum rate of weight loss. Residue at 600°C [%].

Sample	Thermal degradation characteristic [°C]				
	$T_{5\%}$	$T_{50\%}$	$T_{80\%}$	$T_{\max}$	Residue at 600°C [%]
WLI0G	308	393	430	386	6
WLI5G	303	396	433	390	8
WLI10G	298	394	431	390	8
WLI20G	290	395	438	390	11
WLI40G	270	395	447	390	15
lignin	267	567	-	382	48

737

738 **Table 4** The effect of lignin content on the tensile properties of lignin/natural rubber  
739 composites.

COMPOSITE	Tensile strength [MPa]	Elongation at break [%]	Permanent elongation after break [%]
WLI0G	16.25 ± 1.1	717 ± 12	18.1 ± 1.0
WLI5G	15.16 ± 0.4	626 ± 15	15.5 ± 1.1
WLI10G	14.22 ± 1.6	706 ± 15	18.4 ± 0.4
WLI20G	14.39 ± 0.7	733 ± 3	18.2 ± 0.5
WLI40G	8.39 ± 0.7	682 ± 26	21.9 ± 0.5

740

741 **Table 5** The results of hardness, resilience, density and abrasiveness tests for the  
 742 analyzed composites.

COMPOSITE	HARDNESS [°Sh A]	RESILIENCE [%]	DENSITY [g/cm <sup>3</sup> ]	ABRASIVENESS [cm <sup>3</sup> ]
WLI0G	43.6 ± 0.3	58.7 ± 2.0	0.9724 ± 0.0003	0.0899 ± 0.0080
WLI5G	45.5 ± 0.5	57.6 ± 0.8	0.9846 ± 0.0021	0.0847 ± 0.0170
WLI10G	44.3 ± 0.5	57.3 ± 0.9	0.9922 ± 0.0006	0.1179 ± 0.0143
WLI20G	41.2 ± 0.3	52.0 ± 1.1	1.0099 ± 0.0004	0.1469 ± 0.0221
WLI40G	38.3 ± 0.4	38.7 ± 0.7	1.0420 ± 0.0009	0.1999 ± 0.0487

743

744 **Table 6** The results of equilibrium swelling measurements performed on the lignin-  
 745 rubber composites.

COMPOSITE	SWELLING RATIO SR [%]	VOLUME FRACTION $V_{fr}$ [-]	MOLECULAR WEIGHT BETWEEN CROSSLINKS $M_c$ [g/mol]	CROSSLINK DENSITY $v \times 10^{-3}$ [mol/cm <sup>3</sup> ]
WLI0G	$290.8 \pm 3.1$	$0.2374 \pm 0.0026$	$191.6 \pm 2.1$	$5.01 \pm 0.05$
WLI5G	$280.9 \pm 0.3$	$0.2371 \pm 0.0003$	$194.2 \pm 0.2$	$5.07 \pm 0.01$
WLI10G	$278.4 \pm 0.9$	$0.2313 \pm 0.0007$	$200.4 \pm 0.6$	$4.95 \pm 0.01$
WLI20G	$279.9 \pm 1.6$	$0.2156 \pm 0.0011$	$218.2 \pm 1.0$	$4.62 \pm 0.02$
WLI40G	$308.2 \pm 2.9$	$0.1771 \pm 0.0018$	$268.6 \pm 2.6$	$3.88 \pm 0.04$

746

747

748

749

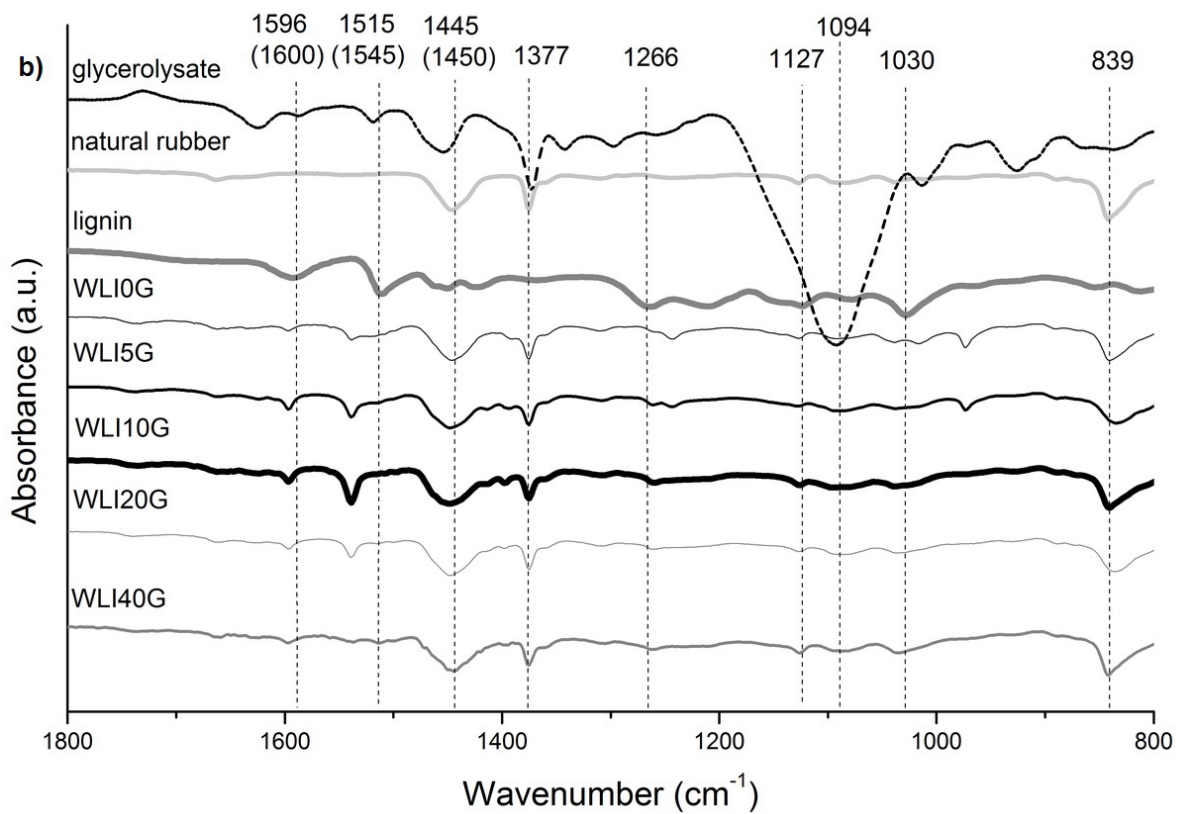
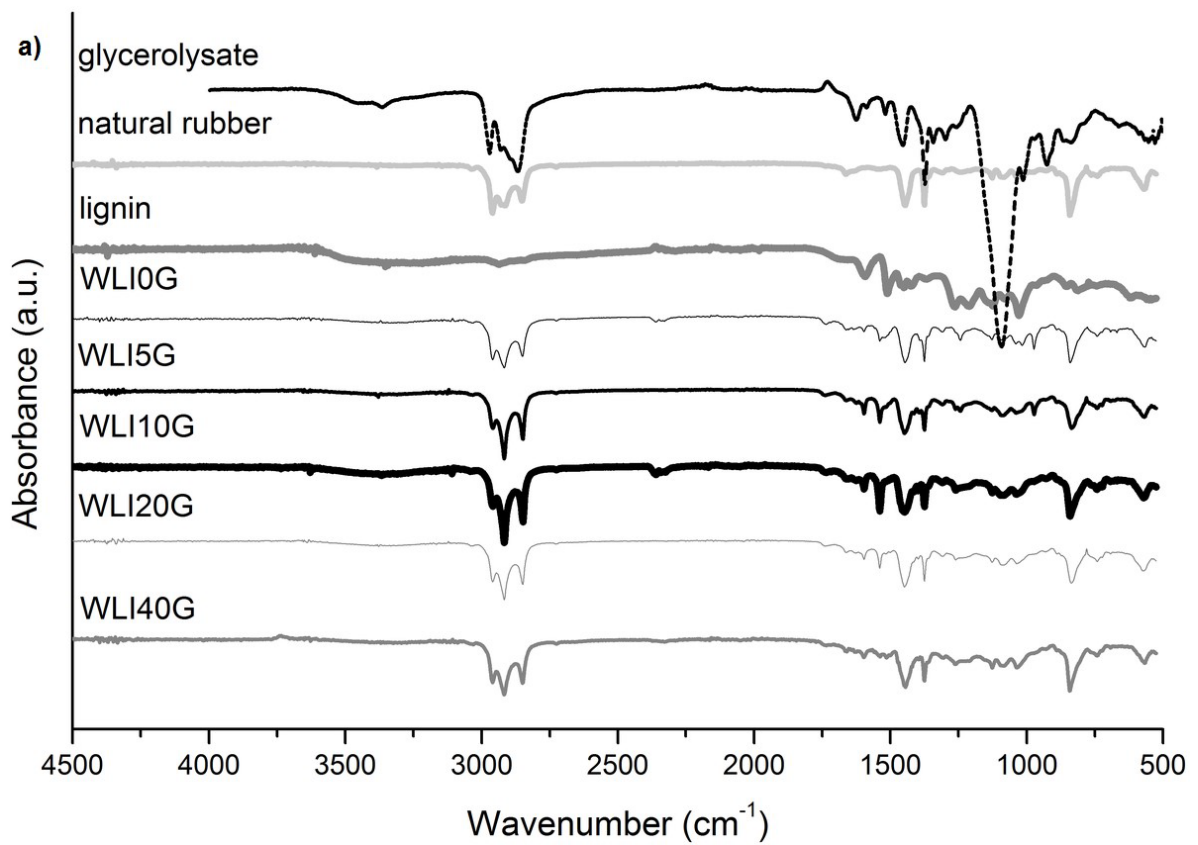
750

751

752

753

754

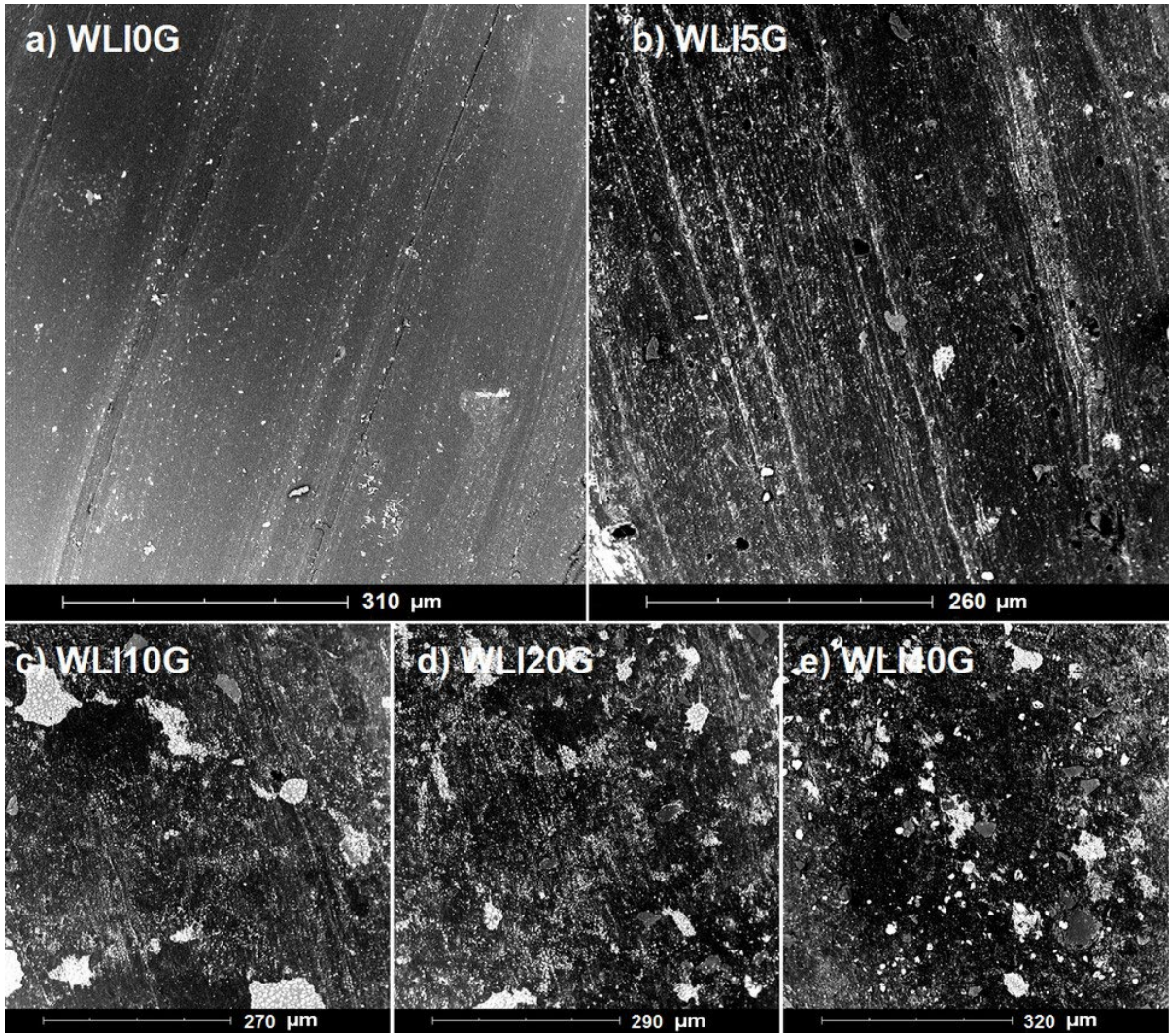


755

756 Figure 1

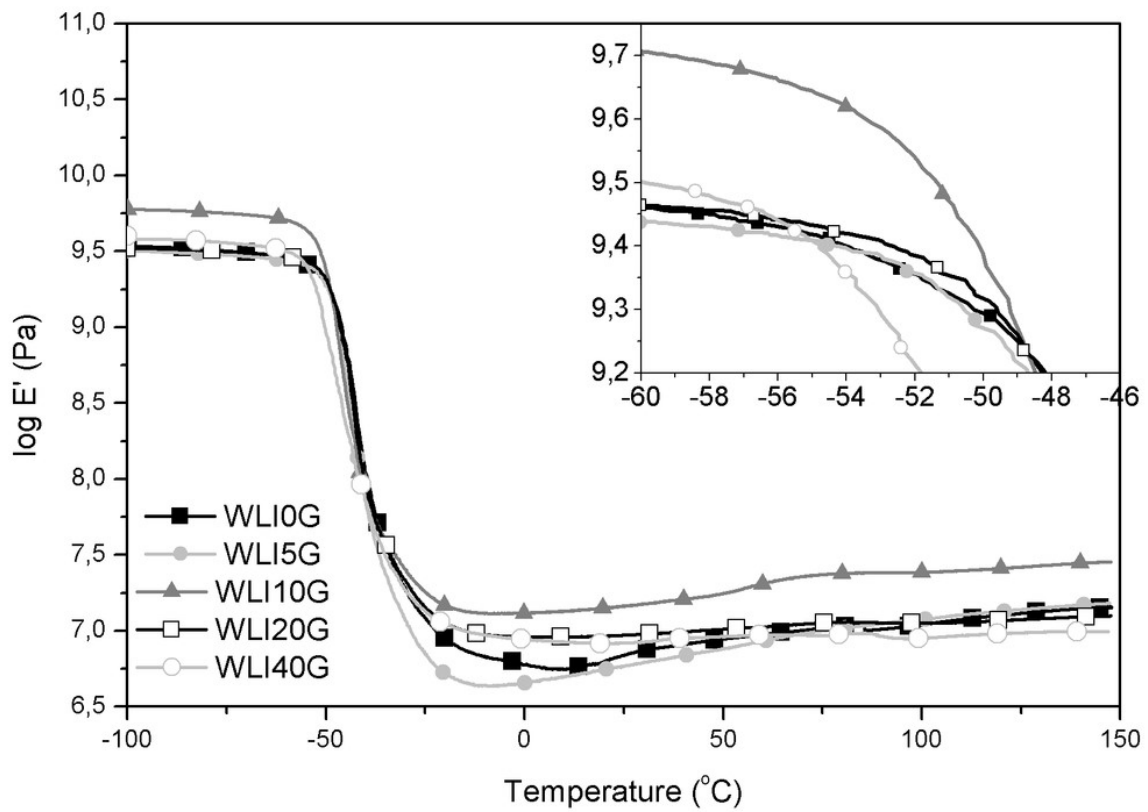
757





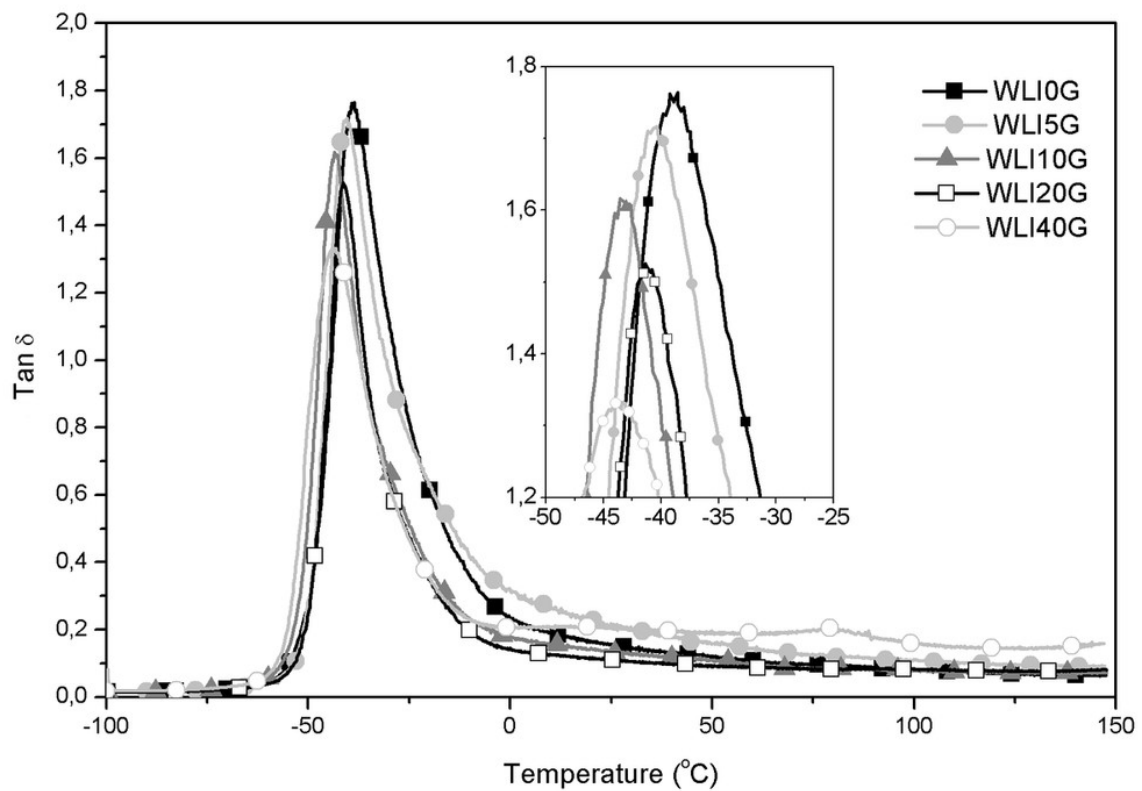
758

759 Figure 2



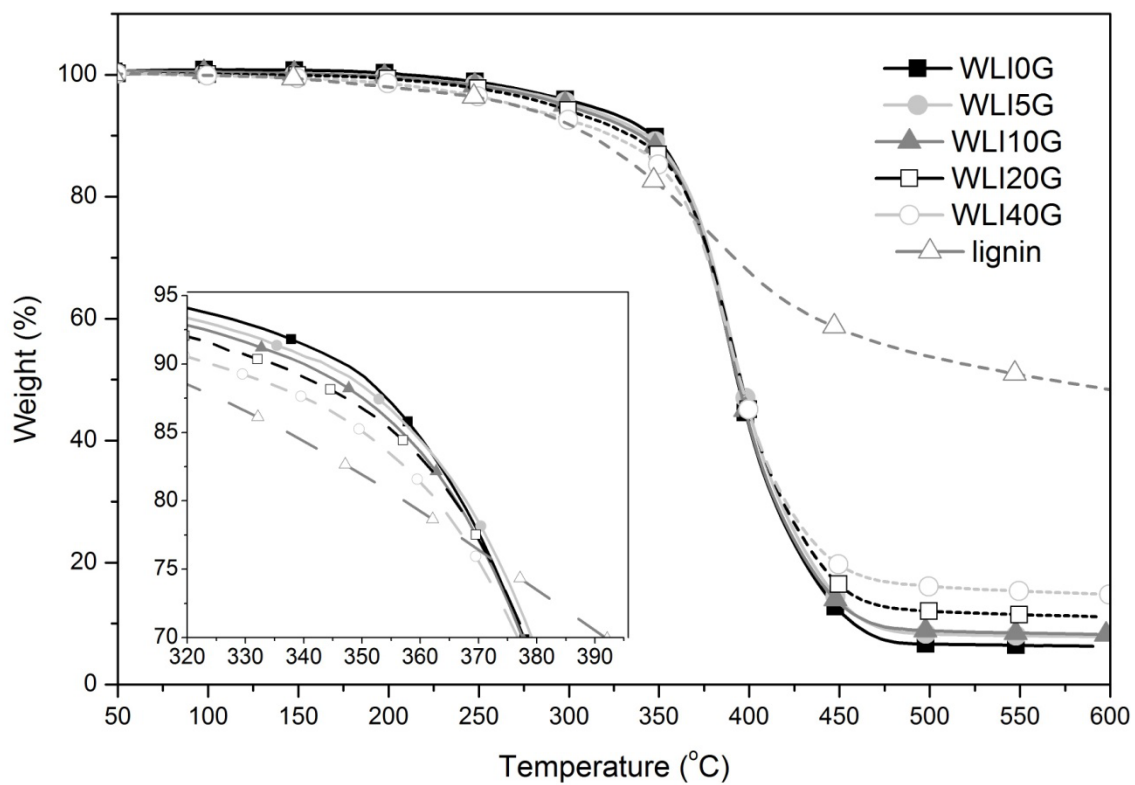
760

761 Figure 3



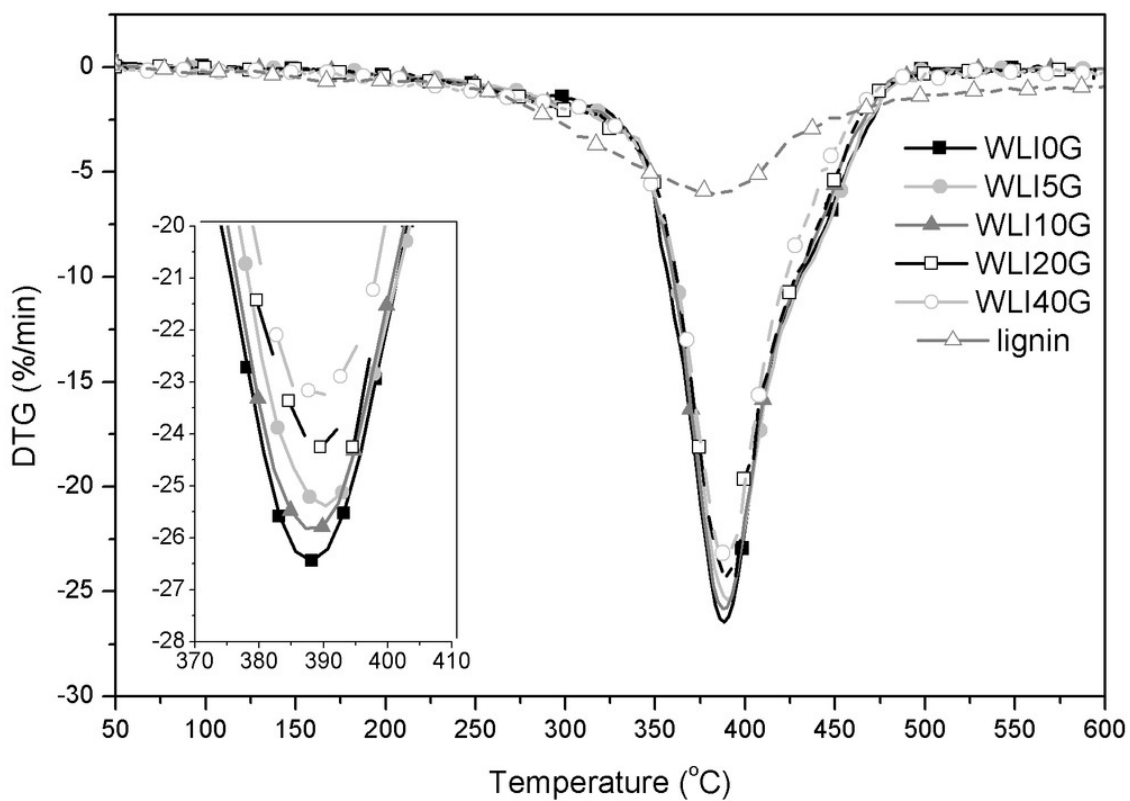
762

763 Figure 4



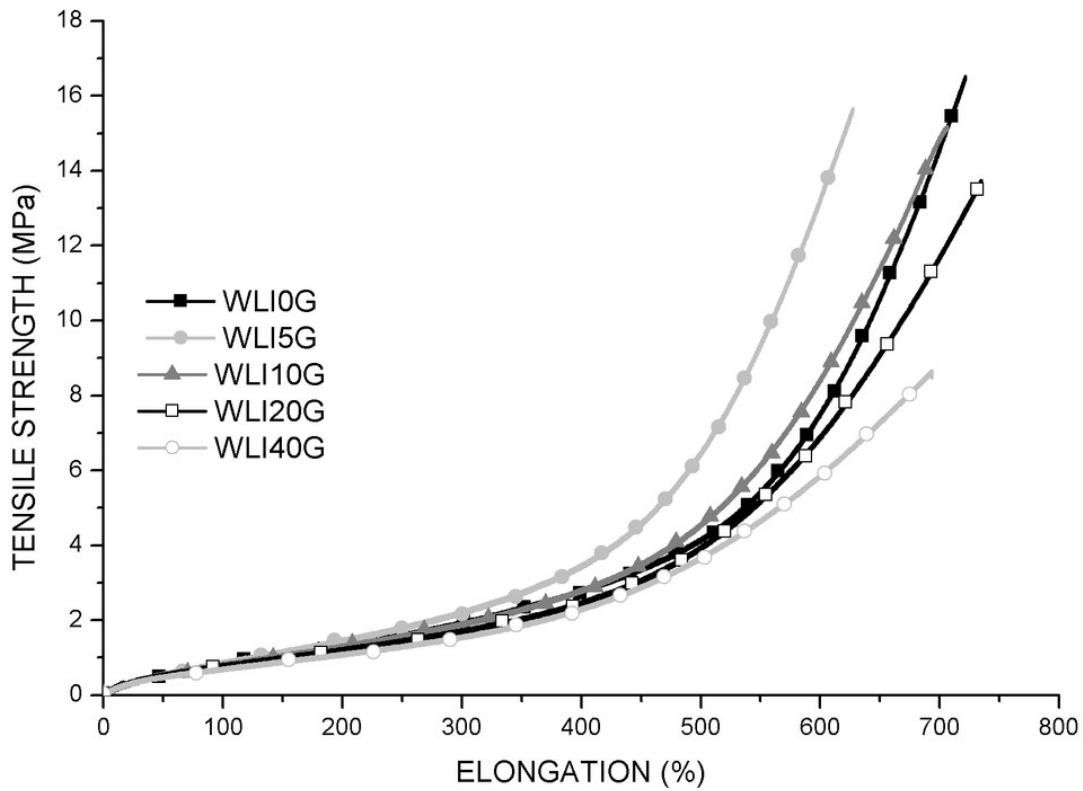
764

765 Figure 5



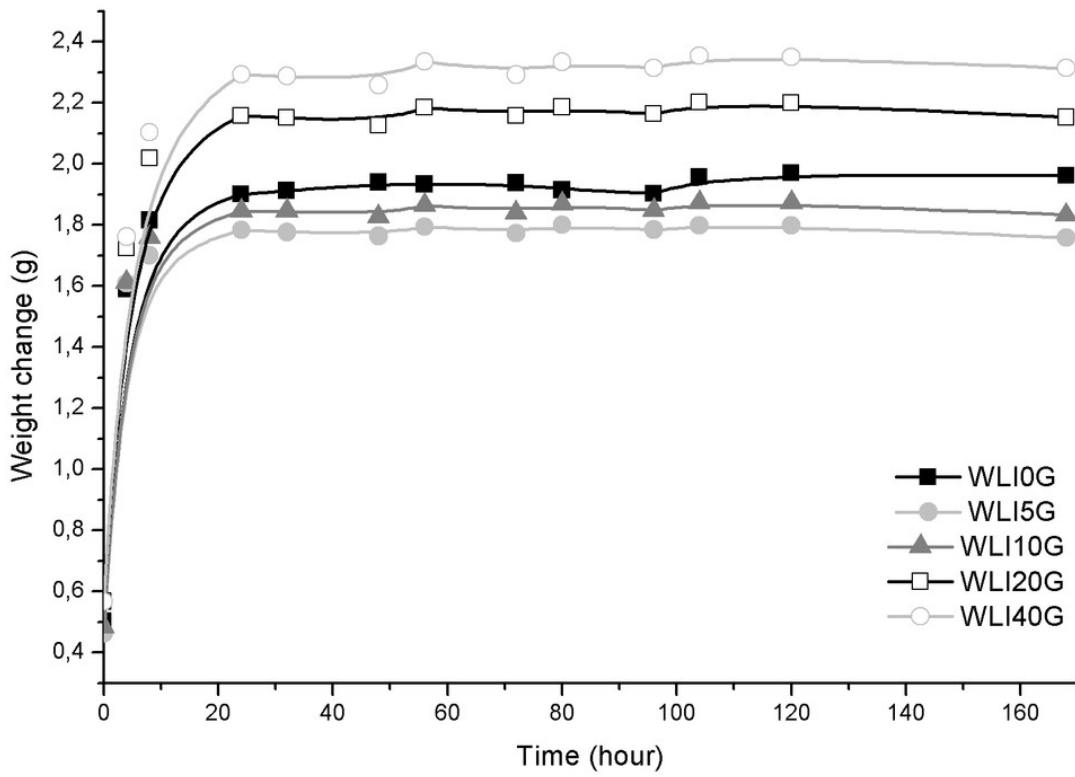
766

767 Figure 6



768

769 Figure 7



770

771 Figure 8